Alumina coatings on silica powders by Fluidized Bed Chemical Vapor Deposition from aluminium acetylacetonate

Philippe Rodriguez, Brigitte Caussat, Xavière Iltis, Carine Ablitzer, Méryl Brothier

Alumina coatings on silica powders by Fluidized Bed Chemical Vapor Deposition from aluminium acetylacetonate

Ph. Rodriguez [a], B. Caussat [b,*], X. Iltis [a], C. Ablitzer [a], M. Brothier [a]

[a] Commissariat à l'Energie Atomique et aux Energies Alternatives, DEN, DEC, SPUA, LCU, Cadarache, F-13108 Saint-Paul-lès-Durance, France
[b] University of Toulouse, ENSIACET/INP Toulouse, LGC – UMR CNRS 5503 4 allée Émile Monso, BP 44362, 31030 Toulouse Cedex, France

HIGHLIGHTS

- The Fluidized Bed Chemical Vapor Deposition process has been studied to coat SiO_2 powder by alumina.
- A metal organic precursor, aluminium acetylacetonate $Al(acac)_3$ has been used as single source.
- Between 400 and 500 °C, the deposits are formed of Al_2O_3, non-decomposed $Al(acac)_3$ and impurities.
- At 600 and 620 °C, the deposits are mainly formed of Al_2O_3 and acetylacetone $C_5H_8O_2$.

Keywords:
CVD
Fluidization
Particle processing
Materials
Alumina
Morphology

ABSTRACT

A SiO_2 powder has been coated by alumina using the Fluidized Bed Chemical Vapor Deposition process and a metal organic precursor, aluminium acetylacetonate ($Al(acac)_3$ or $C_{15}H_{21}AlO_6$) as single source. A range of low temperatures, i.e. 400–620 °C has been explored at atmospheric pressure. Systematic characterizations were performed by Field Emission Gun Scanning Electron Microscopy (FEG-SEM) coupled with Energy Dispersive X-ray Spectroscopy (EDS), Fourier Transform Infra-Red (FT-IR) spectroscopy and Inductively Coupled Plasma Atomic Emission Spectroscopy (ICP-AES). The process involves a first step of gas phase reactions producing reactive intermediates, themselves leading to Al_2O_3 and carbon containing deposits. Between 400 and 500 °C, the deposits are lamellar and constituted of mixtures of Al_2O_3, non-decomposed $Al(acac)_3$ and impurities, leading to a C/Al molar ratio close to 2. For this range of temperature, the precursor is not totally decomposed and the limiting parameter of the process is the deposition temperature. For 600 and 620 °C, the deposits are nodular and mainly formed of Al_2O_3 and acetylacetone $C_5H_8O_2$, one of the main intermediate species formed in the gas phase. The $Al(acac)_3$ decomposition seems to be complete, but a deposition temperature of 620 °C is not high enough to allow a complete decomposition of carbon ligands of the chemisorbing intermediate species. For these conditions, the C/Al molar ratio increases with the deposition temperature, to reach values between 4 and 6, in agreement with the observed darker colors of the deposits.

1. Introduction

The control of surface properties of powders by an appropriate coating is of main concern to enhance their performances for many applications [1]. One of the most efficient technologies to coat the outer surface of powders is the Fluidized Bed Chemical Vapor Deposition (FBCVD) process. CVD offers several advantages compared to wet preparation routes, in particular the absence of solvent and of additional steps of calcination or separation [2]. The Fluidized Bed (FB) is well suited for powders coating due to intense solid mixing, excellent heat and mass transfers and uniform temperatures [3–5]. To illustrate its large range of applications, the FBCVD process has been used to prepare supported catalysts [2], to produce photovoltaic materials [4], to improve surface properties of powders towards wear, oxidation and temperature resistance [5], to coat nuclear fuel particles and to produce multi- or single-walled carbon nanotubes [6].

Alumina coatings have attracted much interest this last decade, due to their interesting physical and chemical properties [7]. Alumina is a relatively hard material, chemically inert and stable at high temperature, which makes it interesting as diffusion barriers [8], or hard coatings [9]. CVD is still today the economically most favorable technique for producing high-quality alumina coatings [10]. Various precursors have been tested including halides or metal organic chemicals like trimethyl aluminium, aluminium

* Corresponding author.
E-mail address: brigitte.caussat@ensiacet.fr (B. Caussat).

http://dx.doi.org/10.1016/j.cej.2012.09.048

tris-isopropoxide or aluminium acetylacetonate. Halides present the disadvantage to produce the aggressive HCl as by-product, resulting in the corrosion of the apparatus and difficulties in handling the exhaust gases [7]. Metal organic precursors are less toxic and allow forming conformal deposits at low temperatures [7,11]. Aluminium acetylacetonate i.e. $Al(acac)_3$ or $Al(C_5O_2H_7)_3$, is a powder at ambient temperature and has a melting point of 192 °C. It is stable under atmospheric conditions, it is relatively easy to handle and it is a commercially available inexpensive compound [7]. Different data of vapor pressure are reported in the literature[7,12,13], leading to quite imprecise results, for instance at 170 °C, 152 Pa for [12] and 759 Pa for [13]. Most literature studies have treated planar substrates and explored ranges of deposition temperatures between 500 and 1000 °C under reduced pressure [7,11,14–20]. Most often, they used vapors of $Al(acac)_3$ mixed with either O_2 or H_2O vapor, in order to decrease the decomposition temperature of the precursor and also to obtain less carbon contaminated films [14–16]. This contamination in carbon is attributed to an incomplete decomposition of $Al(acac)_3$ ligands at the deposition surface. The influence of these decomposition by-products on the deposition rate is unclear. For Devi et al. [14], these products could increase the deposition rate whereas Kim et al. [16] have obtained an opposite conclusion. Some authors [17,18] agree on the fact that this carbon incorporation is favored at low temperature. The chemical mechanisms occurring during CVD from $Al(acac)_3$ are quite complex. Several simplified chemical paths have been proposed [18–20], all involving in a first step gas phase reactions producing intermediates, in particular $Al(C_5H_7O_2)_2OH$ and acetylacetone $C_5H_8O_2$. These intermediates then lead to Al_2O_3 and carbon containing deposits and to the formation of by-products like acetone or H_2O.

Only few works concern CVD of alumina on powders. Johnson and Schilke [21] have combined a plasma enhanced CVD process and a fluidized bed to coat by alumina SiC particles under reduced pressure using argon, oxygen and aluminium tri-sec-butoxide. The group of George and Weimer [22] has used a Fluidized Bed Atomic Layer Deposition process to deposit nanometric layers of alumina on micronic and nanometric particles. Trimethyl aluminium and water vapor have been sequentially injected into the fluidized bed operating under reduced pressure between 75 and 300 °C.

The present work aims to study the Fluidized Bed Chemical Vapor Deposition (FBCVD) process to deposit micronic alumina films at atmospheric pressure on the surface of SiO_2 powders using $Al(acac)_3$ as single-source precursor, in a range of relatively low temperatures, i.e. between 400 and 620 °C.

2. Experimental details

The Fluidized Bed Chemical Vapor Deposition reactor was a vertical cylindrical column of stainless steel, 0.05 m inner diameter (ID) and 1 m height. The reactor was externally heated by a two-zone electrical furnace controlled by a PID regulator connected to two thermocouples fixed on the outer reactor wall. Several thermocouples were also placed into a vertical tube of 6 mm ID along the reactor central axis. An Inconel™ porous plate was used for the gas distribution. All experiments were carried out at atmospheric pressure. A differential pressure sensor measured the pressure drop existing between the bottom part of the reactor (under the distributor) and its top part. Moreover, an absolute pressure gauge allowed monitoring the total pressure above the distributor. A DasyLab® system enabled the on-line acquisition of the differential pressure, the total pressure and the axial profile of bed temperatures.

The alumina coatings were performed using $Al(acac)_3$ (99%) as a single-source Metal Organic (MO) precursor purchased from Strem Chemicals, Inc. During MOCVD experiments, the $Al(acac)_3$ precursor was evaporated from a stainless steel sublimator placed in a thermostated oil bath and was fed into the reactor through heated lines to prevent condensation. Argon flow rates, supplied directly to the bottom of the reactor or through the sublimator, were controlled by mass flow controllers.

The SiO_2 powder provided by Silmer Inc. was sieved before to be coated, in order to tighten its granulometry distribution and to improve its ability to fluidize. After sieving, laser granulometry measurements performed at least three times for each sample (Malvern Master Sizer 2000) indicated that its median diameter d_{50} is of 345 μm. Fig. 1a shows that the granulometry distribution is bimodal and quite large (d_{10}/d_{90} of 90/620 μm). A SEM view of the powder is presented in Fig. 1b where it can be seen that the powder is strongly faceted. Its grain density is of 2,300 kg/m^3. The powder then belongs to the Geldart's group B [23] with however a large size distribution and an angular morphology, not favoring perfect fluidization.

The fluidization hydrodynamics was studied at ambient temperature by measuring the bed pressure drop versus increasing and decreasing gas superficial velocity. A normalized bed pressure drop ΔP^* was calculated by dividing the bed pressure drop measured experimentally by the theoretical one (equal to the bed weight per column cross-sectional area).

The morphology and the composition of the SiO_2 powder and the coated particles were studied by Field Emission Gun Scanning Electron Microscopy (FEG-SEM) coupled with Energy Dispersive X-ray Spectroscopy (EDS) analyses (Philips XL 30 FEG) and by FEG-SEM (JEOL JSM 6700F). Moreover, the chemical composition of the films was analyzed by Fourier Transform Infra-Red (FT-IR) spectroscopy using a Thermo Nicolet Nexus 470 FT-IR spectrometer. The IR spectra were recorded under diffuse reflection conditions in the 4000–400 cm^{-1} region. For each spectrum, the number of scans was 100 and the resolution was 4 cm^{-1}. Film spectra were obtained by subtracting the spectrum of uncoated powder (reference) to spectra obtained for coated powders. Thus, the obtained spectra only correspond to the deposit and not to a combination of the deposit and the substrate. The carbon and aluminium concentrations of the powder before and after CVD were also measured by inductively coupled plasma atomic emission spectroscopy (ICP-AES) (Thermo-Fisher iCAP6300).

For each run, the mass of powders was of 250 g, corresponding to a ratio between the fixed bed height and the column diameter of 2.3. The fluidization ratio, i.e. the ratio between the gas velocity and the minimum fluidization velocity, U/U_{mf} was kept equal to 3 for all runs (U_{mf} being equal to the minimum fluidization velocity measured at ambient temperature). The deposition conditions studied are detailed in Table 1.

3. Results and discussion

3.1. Process behavior

First, the fluidization hydrodynamics was studied in the FBCVD reactor at ambient temperature, using pure argon. The elutriation (loss of powder in the exhaust gas) was negligible. The pressure drop curve (Fig. 2a) shows a hysteresis between the values obtained at increasing and decreasing gas flow rates. This could be related to non-negligible inter-particles forces existing in the FB [24], due to the large diameter distribution of the SiO_2 powder and to their angular shape. However, a fluidization plateau was clearly obtained for a value of the normalized bed pressure drop ΔP^* equal to 1. Using the classical Davidson and Harrison method [25] for the curve obtained at decreasing gas flow rate, a minimum fluidization velocity of 10.2 cm/s was obtained. The bed height expansion was

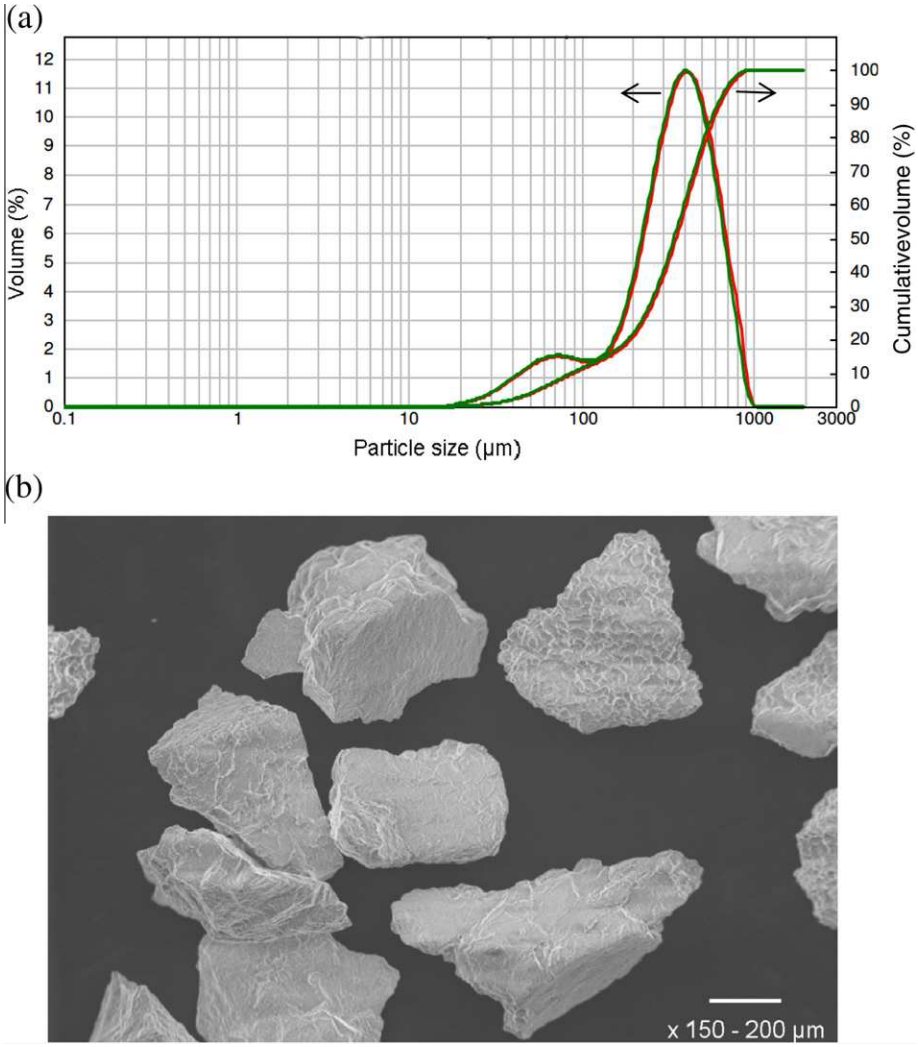

Fig. 1. (a) Volume diameter distribution of the SiO_2 powder. (b) SEM view of the SiO_2 particles.

Table 1
Operating conditions tested.

Run	FB temperature (°C)	Ar flow rate in the sublimator (slm)	Deposit duration (h)	Sublimator temperature (°C)
S1	400	3.3	2	170
S2	400	3.3	2	170
S3	400	3.3	4	170
S4	400	4	2	170
S5	450	4	2	170
S6	500	4	2	170
S7	600	4	2	170
S8	620	4	2	170
S9	620	4	2	175

measured as equal to 25% for 20 cm/s and to 40% for 30 cm/s. These quite high values would lead to good thermal transfers between the reactor wall and the FB particles and also to satisfactory mass transfers between the gas and the fluidized powder.

A characteristic example of thermal profiles measurements into the FB for a fluidization ratio U/U_{mf} of 3 and a target temperature of 500 °C (run S6) is given in Fig. 2b. The thermal gradient along the FB height measured by temperatures TC2 to TC6 was lower than 3 °C, proving that the fluidization of the SiO_2 particles was fully achieved. The temperature TC1 measured in the bottom part of the reactor under the distributor was kept lower than 200 °C in order to avoid any premature decomposition of the precursor.

During CVD experiments, the monitoring of the gas pressure drop across the bed and of the bed temperatures allowed to verify that the fluidization state was maintained. This explains why uniform coatings of powders were systematically obtained, as proved by the numerous SEM and FT-IR spectroscopy analyses performed.

The measured masses of sublimated $Al(acac)_3$ (deduced from the weighing of $Al(acac)_3$ present in the sublimator before and after each experiment) and of the deposits on powders (deduced from the FB weighing before and after each run), are given in Table 2. Due to the unavoidable loss of some FB particles at the end of the runs, the accuracy of these latters is low. The ICP-AES results are also given. The level of detection was of 0.1 wt.% for C

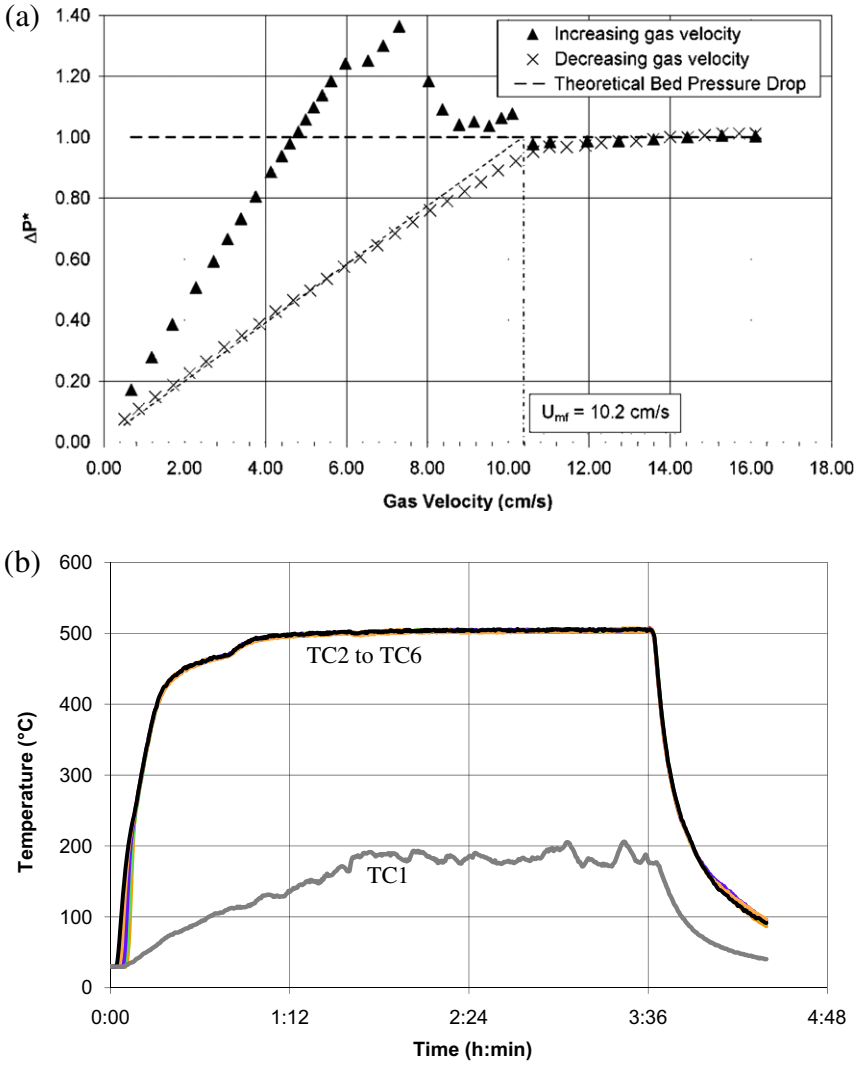

Fig. 2. (a) Pressure drop curve for the SiO_2 powder at increasing and decreasing argon flow rate measured at ambient temperature. (b) Thermal profile measured during run S6 (position of the thermocouples above the distributor: TC2: 1 cm, TC3: 2.5 cm, TC4: 5 cm, TC5: 7 cm, TC6: 9 cm- TC1 is located below the distributor).

Table 2
Experimental results deduced from sublimator and fluidized bed weighing and ICP-AES data.

Run	Mass of sublimated $Al(acac)_3$(g)	Deposition mass on the FB powder (g)	ICP- AES carbon wt.%	ICP- AES aluminum wt.%	C/Al molar ratio	Mass of deposited Al (g)	Mass of sublimated Al (g)	Deposition yield (%)
SiO_2	–	–	<0.1	0.04	–	–	–	–
S1	9.6	1.5	0.14	0.14	2	0.35	0.80	43.8
S2	8.9	1.4	0.11	0.12	2	0.30	0.74	40.5
S3	11.2	1.76	0.21	0.17	2	0.43	0.93	46.2
S4	10	1.57	0.14	0.14	2	0.35	0.83	42.2
S5	10.4	1.63	<0.1	0.25	–	0.63	0.87	72.4
S6	7.6	1.2	0.27	0.21	2	0.53	0.63	84.1
S7	9.7	1.5	0.62	0.31	4.3	0.78	0.81	96.3
S8	9	1.4	0.63	0.26	5.2	0.65	0.75	86.7
S9	13.2	2.1	1.27	0.43	6.3	1.08	1.10	98.2

and of 0.05 wt.% for Al. Regarding the very low measured values, these results only give tendencies. All these data have allowed calculating a molar C/Al ratio and a deposition yield corresponding to the ratio between the masses of deposited Al and of sublimated Al (neglecting the Al percentage present in the non-treated SiO_2 powder).

Let us note that first exploratory experiments have been performed during 1h30 using sublimator temperatures of 120 °C and 130 °C: no sublimation occurred. At 150 °C during 1h30, the sublimated mass was lower than 1 g. We have then fixed the temperature at 170 °C and 175 °C, as detailed in Table 1.

First, runs S1 and S2 correspond to reproducibility experiments. The relative errors on the weights of sublimated $Al(acac)_3$ and of deposits on the FB powders are lower than 8%, showing a good reproducibility of the deposition process. The Al and C contents measured for runs S1 and S2 are low (<0.15 wt.%) and also quite

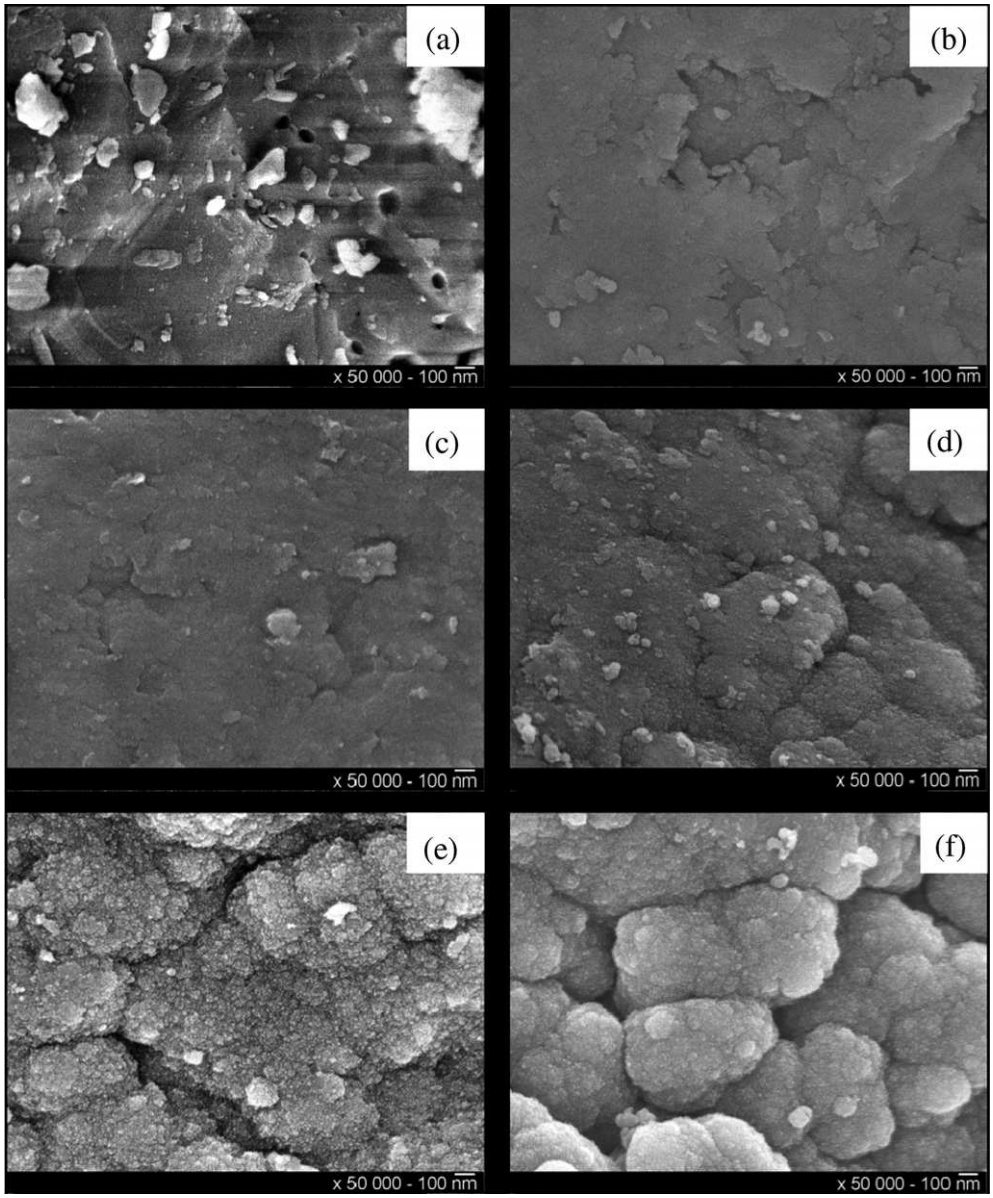

Fig. 3. FEG-SEM views of the powders surface for samples (a) non-treated SiO_2, (b) S5 (c) S6, (d) S7, (e) S8 and (f) S9.

close to each other. They lead to a deposition yield of only 40–43%. These low values are probably due to the low deposition temperature imposed (400 °C), and indicate a weak decomposition of the precursor and consequently a small deposition rate. When comparing the masses of sublimated precursor between runs S4 to S8 for which the sublimation conditions were similar, slight variations of the oil bath temperature and some weighing errors of the precursor after experiments probably explain the observed differences.

The deposition yield clearly increases with the deposition temperature (runs S4 to S8): at 450 °C, it is equal to 72% and reaches 84% at 500 °C and more than 95% from 600 °C. The Al content tends also to increase with the deposition temperature, from 0.14 to 0.25–0.3 wt.%. This trend is more marked for the C content, since for deposition temperatures lower than 600 °C, the C/Al molar ratio into the powder remains close to 2, whereas it is equal to 4 at 600 °C and exceeds 5 at 620 °C. This behavior is a priori in contradiction with some results of the literature [14,17] showing that using $Al(acac)_3$ as precursor, the C incorporation into the deposits is favored by low temperatures. However, the range of temperatures studied in these works is much larger than our (500–1100 °C vs. 400–620 °C), which could explain the opposite conclusions. So, for the conditions tested, increasing the deposition temperature leads to an increase of the deposition yield and probably of the deposition rate, but also of the C content of the deposits.

Table 2 also indicates that doubling the deposit duration (run S3) increases weakly the mass of sublimated precursor. This is probably due to the fact that blocks of $Al(acac)_3$ were observed into the sublimator after all runs, and more importantly after run S3. This means that a degradation of the precursor occurs during its heating at 170 or 175 °C into the sublimator, and that consequently, the sublimation rate decreases with run duration. Logically, the increases of the final FB mass and deposition yield after run S3 are limited when comparing with runs S1/S2. So, the increase of the deposition duration is not the most efficient way to increase the deposition thickness for this process. Higher sublimator temperatures were not tested because of the higher risk of precursor degradation and because of the closeness with the $Al(acac)_3$ melting point (192 °C).

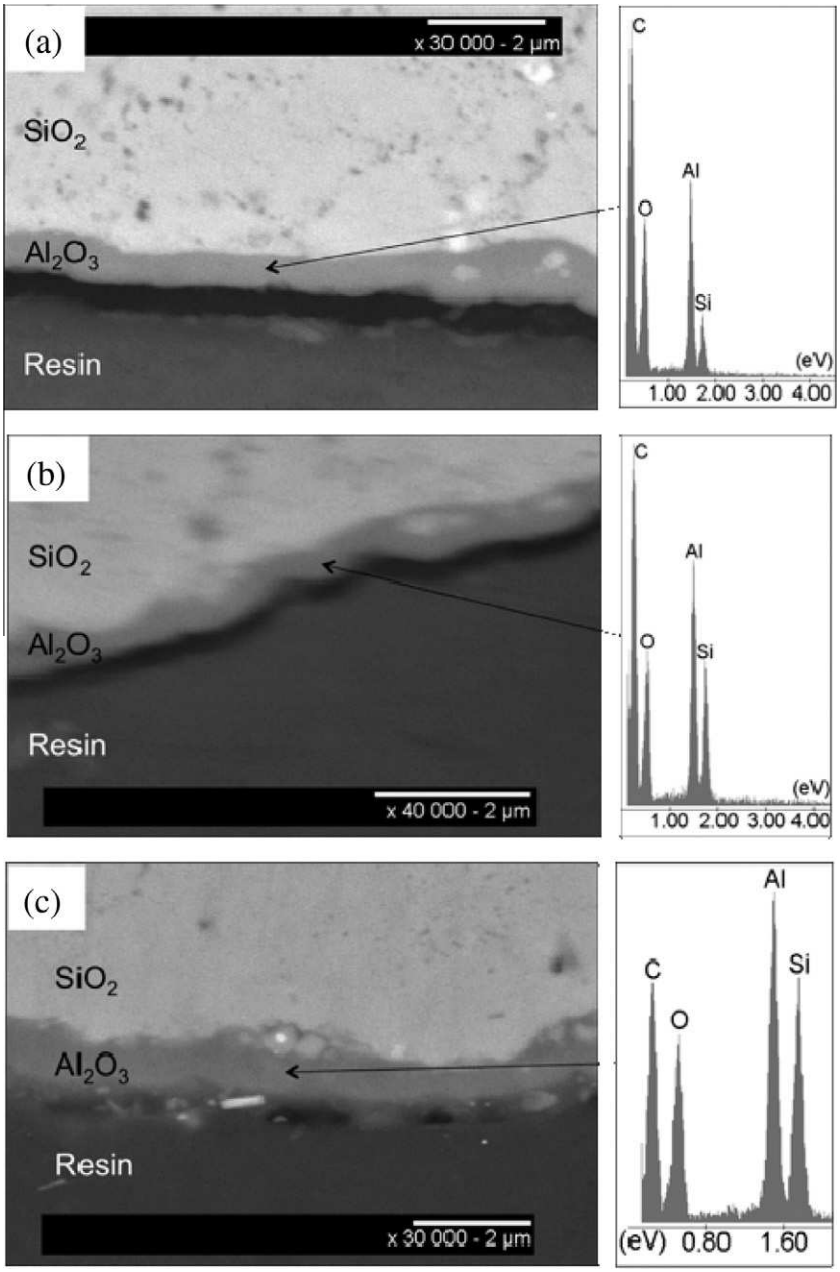

Fig. 4. FEG-SEM views in cross section of polished powders put in a resin and EDS results for samples (a) S7, (b) S8 and (c) S9.

It can also be noted that a moderate increase of the argon flow rate in the sublimator (run S4) has no influence on the deposition results, probably because the saturation conditions were not reached and the limiting step was the sublimation of the precursor.

A confirmation of this assumption can be found by comparing the results of run S9 with those of run S8: an increase of the sublimator temperature of only 5 °C leads to an increase of the sublimated $Al(acac)_3$ mass of more than 4 g and of the deposition mass on the FB powder of 0.7 g. The C and Al percentages in the powder also increase of 30–40% and the C/Al ratio reaches a value close to 6. The deposition yield exceeds 98%. So the fact to have an inlet gas flow rate more concentrated in precursor could generate more intense gas phase reactions forming reactive intermediates and then more intense deposition reactions on the powder.

A first conclusion can be drawn about the fact that the limiting step of the process is mainly temperature between 400 and 500 °C, since the deposition yield (so the precursor decomposition in gaseous intermediates able to chemisorb on the powder surface) increases with the temperature. On the opposite, from 600 °C, the limiting step is mainly the reactive inlet flux, since the deposition yield exceeds 90–95%, so the precursor decomposition is quasi complete, and the Al concentration of the powders and so the deposition rate significantly increase. Higher deposition rates seem to involve higher carbon contents in the deposits, probably due to an incomplete decomposition of the chemisorbing intermediates for this range of low temperatures.

3.2. Morphology of the deposits

First, the colors of powders after deposition are orange-brown for samples S1 to S4, and beyond 450 °C, darker colors are obtained to reach a black tint at 620 °C (samples S8 and S9). Similar colors for alumina deposits from $Al(acac)_3$ have already been reported in the literature [11,17] and have been attributed to the presence

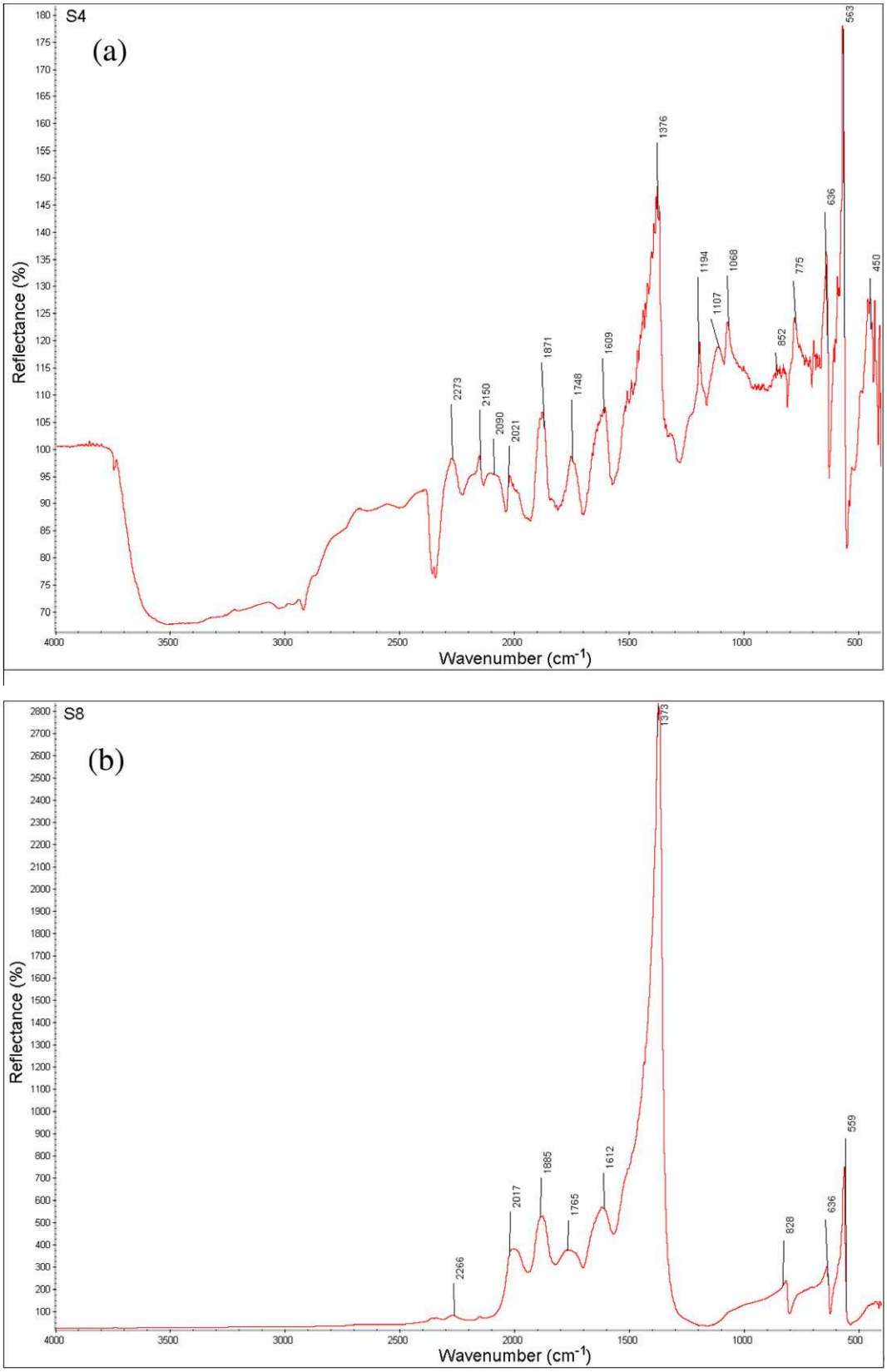

Fig. 5. FT-IR spectra for samples (a) S4 and (b) S8.

of carbonaceous impurities into the deposits. This evolution of color is coherent with the variation of the C/Al ratios previously detailed.

The morphology of the deposits has been studied by FEG SEM, as illustrated in Fig. 3. The surface of the non-treated SiO_2 powder (Fig. 3a) is rather smooth, even if some cavities and asperities are

visible, probably due to the synthesis process of these silica particles. The surface morphology of samples S1 to S6 is quite similar: the surface roughness is low, the deposit seems lamellar even if some nodules of maximum size 100 nm are present, as can be seen in Fig. 3b and 3c for runs S5 and S6. From a deposition temperature of 600 °C, the surface morphology is clearly modified. The deposition no more occurs under the form of bi-dimensional plates but of spheroidal nodules. The tri-dimensional nature of the deposits increases with the deposition temperature and also with the sublimator temperature, as illustrated in Fig. 3d–f for runs S7–S9. At 620 °C, the deposit has cauliflower morphology. A possible mechanism could be that the gas phase decomposition of the $Al(acac)_3$ increases with the deposition temperature, leading to higher flux of reactive intermediate species arriving on the powder surface. Beyond a critical flux, the ad-atoms diffusion on the surface is not rapid enough to maintain a bi-dimensional deposition, and then tri-dimensional nodules appear. It is worth noting that this tri-dimensional morphology is observed for the deposits presenting the highest C/Al molar ratios, i.e. between 4 and 6. So, the temperatures of 600 and 620 °C are high enough to allow a more intense chemisorption of the intermediates on the powder surface, but they are not sufficient to completely decompose the carbon ligands of the intermediates.

3.3. Uniformity and thickness of the deposits

In order to analyze the uniformity and thickness of the deposits around the SiO_2 powder, FEG-SEM observations in cross section have been performed on polished powders put in a resin using a backscattered electron (BSE) detector to highlight the contrast between areas presenting different chemical compositions.

The deposits on samples S1–S6 could not be observed, probably because they are too thin. For samples S7–S9, numerous analyses have been performed, showing a good uniformity of the deposits around each SiO_2 particle and on the whole powder surface. Fig. 4 gives examples of FEG SEM micrographies and of EDS measurements performed in the zones of the deposits. They show the presence of Al, O and C. Silicon also appears because the EDS analyses concern volumes close to 1 μm^3 and the deposit thicknesses are lower than 1 μm. A mean thickness of 0.7 ± 0.1 μm has been measured for sample S7, 0.5 ± 0.1 μm for S8 and 0.9 ± 0.1 μm for S9. The values obtained for S7 and S8 are quite close of each other, probably because of the quite low difference of deposition temperature (20 °C) and of a sublimated mass of precursor slightly higher for run S7. Sample S9 presents the highest thickness obtained, which confirms the positive effect of an increase of the sublimation temperature, so of the precursor inlet flux, on the deposition rate for the tested conditions.

3.4. Chemical composition of the deposits

Some FT-IR measurements have been performed on all samples. The FT-IR results can be classified in two groups, samples S1–S6 on one hand and S7–S9 on the other hand. The main difference between the two groups is the deposition temperature: it is comprised between 400 and 500 °C for the first one, and it is equal to 600–620 °C for the second one. Characteristic spectra of the results obtained are given for samples S4 and S8 in Fig. 5. To refine their analysis, spectra have been compared with the IR reference spectra of $Al(acac)_3$ and of one of its main decomposition by-products under argon, acetylacetone $C_5H_8O_2$ [20].

First, when comparing spectra of all experiments, their intensity increases with the deposition temperature and the flux of injected precursor. This phenomenon can probably be linked to an increase of the deposit thicknesses.

Much more vibration peaks are present on the S1–S6 spectra than on the S7–S9 ones. This could be due to the presence of more impurities in the deposits of S1–S6 samples. The peaks observed between 1400 and 1650 cm^{-1} could be attributed to carbon species since they are characteristic of C═C and C—O bonds [26]. The peaks at 690, 775 and 1,190 cm^{-1} could be related to non-decomposed $Al(acac)_3$ molecules adsorbed in the deposit. They tend to disappear with an increase of deposition temperature, which confirms an incomplete decomposition of $Al(acac)_3$ at temperatures lower than 600 °C. The peaks beyond 2,000 cm^{-1} have not been clearly attributed; they could be linked to the deposition of homogeneously formed by-products containing triple C≡C bonds.

A peak close to 1615–1620 cm^{-1} is present for sample S4 and has a growing intensity with the deposition temperature. It probably corresponds to the most intense peak of the acetylacetone spectrum. This confirms that for all the deposition temperatures tested, the deposit is a mixture of alumina and of homogeneously formed intermediates.

For samples S7–S9, the peaks characteristic of $Al(acac)_3$ are no more present, which confirm that from 600 °C, the precursor is totally decomposed in intermediate species. This result is coherent with the observations detailed in Section 3.1. Another peak is present on the S7–S9 spectra, close to 2,000 cm^{-1} whose origin has not been identified.

Numerous peaks between 500 and 1000 cm^{-1} are common to the whole analyzed samples and are probably linked to alumina. The peak between 630 and 800 cm^{-1} can be attributed to the bending vibration of the O—Al—O bond [26]. The peak between 810 cm^{-1} and 1000 cm^{-1} could correspond to the stretching vibration of the Al—O bond [27].

The peak close to 1370 cm^{-1} is the most intense one for samples S5 to S9, and its intensity is increasing from samples S2 to S9. It could be linked to the reference spectrum of the acetylacetone and probably correspond to the vibration of CH_3 aliphatic groups. In this case, the fact that this peak has an increasing intensity with the deposition temperature could indicate that the main intermediate formed by the gas phase decomposition of $Al(acac)_3$ and chemisorbing on the powder surface is acetylacetone.

4. Conclusion

The Fluidized Bed Chemical Vapor Deposition process has been studied at atmospheric pressure to coat SiO_2 powder by alumina using a metal organic precursor, aluminium acetylacetonate $Al(acac)_3$ as single source. A range of low temperatures, i.e. 400–620 °C has been explored.

The ability to fluidize of the SiO_2 powder and the good temperature uniformity existing in the fluidized bed have been first verified. Then, the deposition results confirm the chemical mechanisms proposed in the literature, i.e. a first step of gas phase reactions producing reactive intermediates themselves leading to Al_2O_3 and carbon containing deposits.

Indeed, between 400 and 500 °C, the deposits are constituted of mixtures of Al_2O_3, non-decomposed $Al(acac)_3$ and impurities, leading to a C/Al molar ratio close to 2. The deposits have a lamellar morphology, involving a bi-dimensional deposition mechanism. The ratio between the injected Al and the deposited Al on the powder surface, i.e. the deposition yield, is lower than 85% and increases with the temperature. So, for this range of temperature, the precursor is not totally decomposed and the limiting parameter of the process is the deposition temperature.

For 600 and 620 °C, the deposits are mainly formed of Al_2O_3 and acetylacetone $C_5H_8O_2$, which seems to be the main intermediate species formed in the gas phase from the decomposition of $Al(acac)_3$ able to chemisorb on the powder surface. The $Al(acac)_3$

decomposition seems to be complete, since the FT-IR analyses have not detected its presence in the deposits. For these conditions, the C/Al molar ratio increases with the deposition and sublimation temperatures, to reach values between 4 and 6, which is coherent with the observed darker colors of the deposits. The deposits are nodular corresponding to a tri-dimensional deposition mechanism, probably because higher fluxes of reactive intermediates are formed due to a more intense $Al(acac)_3$ gas phase decomposition, exceeding the kinetics of ad-atoms surface diffusion. At 620 °C, an increase from 170 to 175 °C of the sublimation temperature leads to a clear increase of the deposit thickness showing that the limiting parameter of the process is in this case the reactive inlet flux. So, the classical CVD behavior of a limitation by chemical reactions at low temperature and by reactive supplying at high temperature is found for this FBCVD process. However, a deposition temperature of 620 °C is not high enough to allow a complete decomposition of carbon ligands of the chemisorbing intermediate species.

Acknowledgements

The authors would like to thank Michel Molinier and Étienne Prevot from LGC for their technical support, Hélène Rouquette and Nicolas Tarisien from CEA for the SEM observations, Joël Raynal and Noëlle Arnaud from CEA for the FT-IR analyses.

References

[1] J.R. Scheffe, A. Frances, D.M. King, X. Liang, B.A. Branch, A.S. Cavanagh, S.M. George, A.W. Weimer, Atomic layer deposition of iron (III) oxide on zirconia nanoparticles in a fluidized bed reactor using ferrocene and oxygen, Thin Solid Films 517 (2009) 1874–1879.
[2] R. Naumann d'Alnoncourt, M. Becker, J. Sekulic, R.A. Fisher, M. Muhler, The preparation of Cu/Al_2O_3 catalysts via CVD in a fluidized-bed reactor, Surf. Coat. Technol. 201 (2007) 9035–9039.
[3] G.S. Czok, J. Werther, Liquid spray vs. gaseous precursor injection – its influence on the performance of particle coating by CVD in the fluidized bed, Powder Technol. 162 (2006) 100–110.
[4] S. Balaji, Juan Du, C.M. White, B. Erik Ydstie, Multi-scale modeling and control of fluidized beds for the production of solar grade silicon, Powder Technol. 199 (2010) 23–31.
[5] J. Perez-Mariano, K.H. Lau, E. Alvarez, R. Malhotra, M. Hornbostel, Multilayer coatings for corrosion protection of coal gasifier components, Mater. Chem. Phys. 112 (2008) 180–185.
[6] C. Vahlas, B. Caussat, Ph. Serp, G.N. Angelopoulos, Principles and applications of CVD powder technology, Mater. Sci. Eng. R 53 (2006) 1–72.
[7] C. Pflitsch, A. Muhsin, U. Bergmann, B. Atakan, Growth of thin aluminium oxide films on stainless steel by MOCVD at ambient pressure and using a hot-wall CVD-setup, Surf. Coat. Technol. 201 (2006) 73–81.
[8] N. Bahlawane, S. Blittersdorf, K. Kohse-Höinghaus, B. Atakan, J. Müller, Investigation of CVD processes to perform dense α-alumina coating on superalloys, J. Electrochem. Soc. 151 (2004) C182–C186.
[9] J.E. Sundgren, H.T.G. Hentzell, A review of the present state of art in hard coatings grown from the vapor phase, J. Vac. Sci. Technol. A 4 (1986) 2259–2280.
[10] S. Canovic, B. Ljungberg, M. Halvarsson, CVD TiC/alumina multilayer coatings grown on sapphire single crystals, Micron 42 (2011) 808–818.
[11] M.P. Singh, S.A. Shivashankar, Low pressure MOCVD of Al_2O_3 films using aluminium acetylacetonate as precursor: nucleation and growth, Surf. Coat. Technol. 161 (2002) 135–143.
[12] R. Teghil, D. Ferro, L. Bencivenni, M. Pelino, A thermodynamic study of the sublimation processes of aluminium and copper acetylacetonates, Thermochim. Acta 44 (1981) 213–222.
[13] A. Siddiqi, R.A. Siddiqi, B. Atakan, Thermal stability, sublimation pressures and diffusion coefficients of some metal acetylacetonates, Surf. Coat. Technol. 201 (2007) 9055–9059.
[14] A. Devi, S.A. Shivashankar, A.G. Samuelson, MOCVD of aluminium oxide films using aluminium β-diketonates as precursors, J. Phys. IV 12 (2002) 139–146.
[15] T. Maruyama, S. Arai, Aluminium oxide thin films prepared by chemical vapor deposition from aluminium acetylacetonate, Appl. Phys. Lett. 60 (1992) 322–323.
[16] J.S. Kim, H.A. Marzouk, P.J. Reucroft, J.D. Robertson, C.E. Hamrin Jr, Fabrication of aluminium oxide thin films by a low pressure metal organic chemical vapor deposition technique, Appl. Phys. Lett. 61 (1993) 681–683.
[17] C. Pflitsch, D. Viefhaus, U. Bergmann, B. Atakan, Organometallic vapour deposition of crystalline aluminium oxide films on stainless steel substrates, Thin Solid Films 515 (2007) 3653–3660.
[18] J. Von Hoene, R.G. Charles, W.M. Hickam, Thermal decomposition of metal acetylacetonates: mass spectrometer studies, J. Phys. Chem. 62 (1958) 1098–1201.
[19] V.G. Minkina, Study of the pyrolysis kinetics of aluminium acetylacetonate in the gaseous phase, Inorg. Mater. 29 (1993) 1400–1401.
[20] M.C. Rhoten, T.C. Devore, Evolved gas phase analysis investigation in the reaction between Tris(2,4-pentanedionato)aluminium and water vapour in chemical vapor deposition processes to produce alumina, Chem. Mater. 9 (1997) 1757–1764.
[21] G.F. Johnson, P.W. Schilke, Alumina coated silicon carbide abrasive, US patent 4, 249, 913 (1981)
[22] X., Liang, L.F. Hakim, G.D. Zhan, J.A. Mc Cormick, S.M. George, A.W. Weimer, J.A. Spencer II, K.J. Buechler, C.J. Wood, J.R. Dorgan, Novel processing to produce polymer/ceramic composites by atomic layer deposition, J. Am. Ceram. Soc. 90 (2007) 57–63. and references therein.
[23] D. Geldart, Types of gas fluidization, Powder Technol. 7 (1973) 285–292.
[24] M.W. Weber, C.M. Hrenya, Computational study of pressure-drop hysteresis in fluidized beds, Powder Technol. 177 (2007) 170–184.
[25] J.F. Davidson, D, Fluidised Particles, Cambridge University Press, Harrison, 1963.
[26] Q.Y. Nguyen, J.N. Kidder, S.H. Ehrman, Hybrid gas to particle conversion and chemical vapor deposition for the production of porous alumina films, Thin Solid Films 410 (2002) 42–52.
[27] A. Ortiz, J.C. Alonso, High quality low temperature aluminium oxide films deposited by ultrasonic spray pyrolysis, J. Mater. Sci. – Mater. Electron. 13 (2002) 7–11.